

# Activation of Ene-Diamido Samarium Methoxide with Hydrosilane for Selectively Catalytic Hydrosilylation of Alkenes and Polymerization of Styrene: an Experimental and Theoretical Mechanistic Study

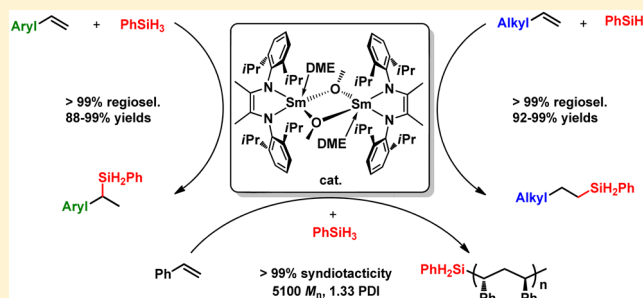
Jianfeng Li,<sup>†</sup> Chaoyue Zhao,<sup>†</sup> Jinxi Liu,<sup>†</sup> Hanmin Huang,<sup>†</sup> Fengxin Wang,<sup>†</sup> Xiufang Xu,<sup>\*,†</sup> and Chunming Cui<sup>\*,†,‡</sup>

<sup>†</sup>State Key Laboratory of Elemento-Organic Chemistry, Nankai University, Tianjin 300071, P. R. China

<sup>‡</sup>Collaborative Innovation Center of Chemical Science and Engineering, Tianjin 300071, P. R. China

## Supporting Information

**ABSTRACT:** Samarium methoxide incorporating the ene-diamido ligand L(DME)Sm( $\mu$ -OMe)<sub>2</sub>Sm(DME)L (**1**; L = [DipNC(Me)C(Me)NDip]<sup>2-</sup>, Dip = 2,6-*i*Pr<sub>2</sub>C<sub>6</sub>H<sub>3</sub>, and DME = 1,2-dimethoxyethane) has been prepared and structurally characterized. Complex **1** catalyzed the syndiospecific polymerization of styrene upon activation with phenylsilane and regioselective hydrosilylation of styrenes and nonactivated terminal alkenes. Unprecedented regioselectivity (>99.0%) for both types of alkenes has been achieved with the formation of Markovnikov and anti-Markovnikov products in high yields, respectively, whereas the polymerization of styrene resulted in the formation of syndiotactic silyl-capped oligostyrenes. The kinetic experiments and density functional theory calculations strongly support a samarium hydride intermediate generated by  $\sigma$ -bond metathesis of the Sm–OMe bond in **1** with PhSiH<sub>3</sub>. In addition, the observed regioselectivity for hydrosilylation and polymerization is consistent with the calculated energy profiles, which suggests that the bulky ene-diamido ligand and samarium hydride intermediate have important roles for regio- and stereoselectivity.



## INTRODUCTION

Well-defined rare-earth complexes have emerged as powerful catalysts for a number of transformations given their unique selectivity and mechanistic distinctions derived from the high electrophilicity of rare-earth centers.<sup>1</sup> Because both catalytic hydrosilylation and polymerization of alkenes are important industrial processes for the production of organosilanes and polyolefins, the reactions catalyzed by rare-earth and early-transition-metal complexes have been studied extensively in the past several decades.<sup>2,3</sup> The most distinctive and attractive features that have been observed for the rare-earth-catalyzed reactions include the following: (1) hydrosilylation of styrenes and nonactivated alkenes yielded products with reverse regioselectivity; (2) polymerization may proceed in the absence of an expensive cocatalyst, like methylaluminoxane.

The most widely employed catalytic precursors for hydrosilylation are rare-earth alkyls supported by various ligand frameworks.<sup>4</sup> Some rare-earth hydrides and amides have also been reported.<sup>5,6</sup> However, these catalysts or precatalysts, especially hydrides and alkyl complexes, suffer from high sensitivity to air and moisture and thus cannot be stored for a relatively long time and are not practical. In addition, the factors that control the regioselectivity of rare-earth-catalyzed

hydrosilylation of alkenes are currently not clear. On the other hand, although a number of rare-earth alkyls and amides have been reported to catalyze the hydrosilylation reactions, only the rare-earth amide La[N(SiMe<sub>3</sub>)<sub>2</sub>]<sub>3</sub> has been reported to exhibit the relatively satisfactory regioselectivity for both aryl-substituted (99%) and alkyl-substituted (96%) terminal alkenes.<sup>6c</sup> This issue has been complicated by the fact that both rare-earth hydride and silyl intermediates could be generated in the catalytic cycle upon the activation of rare-earth alkyls and hydrides with hydrosilanes, leading to the insertion of alkenes into either rare-earth hydride or silyl intermediates.<sup>7</sup>

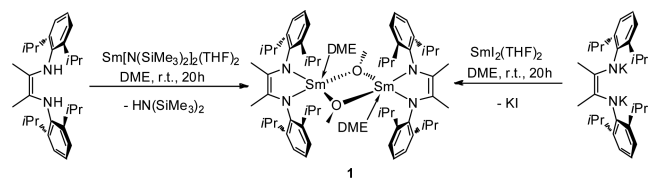
Trivalent rare-earth alkoxides/aryloxides are well-known to be much more resistant to air and moisture and thus much easier to handle and store for a long time. However, they have not been reported as hydrosilylation and polymerization catalysts of alkenes because of the large Ln–O bond enthalpy,<sup>8</sup> which impedes the formation of active hydride or silyl intermediates via  $\sigma$ -bond metathesis with hydrosilane. This situation is in sharp contrast to that of transition-metal

Received: July 19, 2016

alkoxides, which, in some cases, could be converted to the corresponding active hydride intermediate by  $\sigma$ -bond metathesis with hydrosilanes.<sup>9</sup> Nevertheless, recent studies by the Marks and Hou groups have shown that the insertion of an Ln–O bond into C=C and C=O bonds could occur under certain conditions.<sup>10,11</sup> Inspired by the successes, we are interested in the investigation of  $\sigma$ -bond metathesis of an Ln–OR bond supported by suitable ligand frameworks with hydrosilanes for the development of practical rare-earth alkoxide catalysts for hydrosilylation reactions.

Herein, we report the selective catalytic hydrosilylation and polymerization of styrenes with the samarium alkoxide **1** incorporating the bulky ene-diamido ligand (Scheme 1) by

### Scheme 1. Synthesis of **1**



controlling the amount of hydrosilane. Complex **1** appeared to be the most regioselective catalyst for hydrosilylation of both styrenes and nonactivated alkenes reported so far. In addition, polymerization of styrene led to the formation of silyl-capped, highly syndiotactic polystyrene. The combined experimental results and density functional theory (DFT) calculations on the mechanisms disclosed the highly selective formation of the samarium hydride intermediate by activation of the Sm–OMe bond, with hydrosilane and the electronic and steric factors of the ene-diamido ligand being responsible for the high regioselectivity for hydrosilylation and stereoselective polymerization of styrene.

## RESULTS AND DISCUSSION

Rare-earth complexes supported by ene-diamido ligands have been shown to display interesting coordination chemistry and reactivity.<sup>12</sup> Their catalytic applications for the polymerization of cyclic esters and 4-vinylpyridine have been reported by Trifonov, Carpentier, and Mashima.<sup>13,14</sup> In addition, yttrium ene-diamido alkyl and hydrido complexes has been reported by Trifonov to catalyze intermolecular olefin hydrophosphination and hydroamination.<sup>15</sup> More recently, we reported the synthesis and reactions of yttrium complexes supported by a bulky ene-diamido ligand.<sup>16</sup> In a continuation of our studies on rare-earth chemistry with redox-active ene-diamido ligands, rare-earth alkoxides supported by dianionic ligands have been chosen for this study.

The methoxy-bridged complex  $[L(DME)Sm(\mu\text{-OMe})]_2$  (**1**; L = [DippNC(Me)C(Me)NDipp]<sup>2-</sup>, Dipp = 2,6-*i*Pr<sub>2</sub>C<sub>6</sub>H<sub>3</sub>, and DME = 1,2-dimethoxyethane) was easily obtained by the reaction of LH<sub>2</sub> with Sm[N(SiMe<sub>3</sub>)<sub>2</sub>]<sub>2</sub>(THF)<sub>2</sub> (THF = tetrahydrofuran) in DME. Complex **1** was isolated as brown crystals in ca. 46% yield. Alternatively, complex **1** can also be prepared by the reaction of the potassium salt LK<sub>2</sub> with SmI<sub>2</sub>(THF)<sub>2</sub> and has been characterized by <sup>1</sup>H and <sup>13</sup>C NMR spectroscopy and elemental analysis. The molecular structure of **1** has been determined by single-crystal X-ray analysis.

Complex **1** displays the broad proton resonances in the wide range from –3.56 to +11.57 ppm in the <sup>1</sup>H NMR spectrum, indicating the paramagnetic nature of the trivalent samarium

ion. The structure of **1** features a crystallographic central symmetry with a Sm1–O4–Sm1\*–O4\* planar core (Figure 1). The C6–C11 bond length of 1.373(3) Å is lengthened

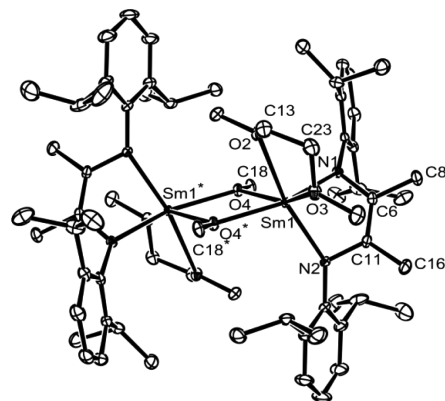


**Figure 1.** ORTEP drawing of **1** with 30% probability. Hydrogen atoms have been omitted for clarity. Selected bond lengths (Å) and angles (deg): Sm1–N1 2.2816(15), Sm1–N2 2.2783(16), Sm1–O2 2.6011(13), Sm1–O3 2.5768(13), Sm1–O4 2.3104(13), Sm1–O4\* 2.3548(12), Sm1–C6 2.8232(18), Sm1–C11 2.8195(19), Sm1–Sm1\* 3.8579(6), N1–C6 1.417(2), N2–C11 1.428(2), C6–C11 1.373(3); N1–Sm1–N2 79.52(5), O4–Sm1–O4\* 68.43(5), Sm1–O4–Sm1\* 111.57(5), N1–Sm1–O4 89.17(5).

compared to the corresponding distance [1.339(2) Å] in the ene-diamine LH<sub>2</sub>.<sup>17</sup> The short distances (av. 2.821 Å) between the samarium and two olefinic carbon atoms and the folded N–C–C–N–Sm five-membered ring (the dihedral angle of the N–Sm–N and N–C–C–N planes = 132.2°) indicated the  $\sigma^2, \pi$ -coordination mode of the ene-diamido ligand.<sup>12b–d,13</sup>

The mechanism for the formation of the trivalent samarium dimer **1** from the divalent precursors is very likely through the divalent samarium ene-diamido intermediate, which is highly reactive and cleaved the C–O bonds in DME molecules via an electron-transfer process. The cleavage of the C–O bond in ether has precedents with trivalent rare-earth metal alkyl, hydride, and halide, as well as an in situ generated divalent rare-earth metal intermediate.<sup>15,18,19</sup> In the latter case, an electron-transfer process has been proposed. The formation of **1** represents a convenient route for the preparation of rare-earth methoxide.

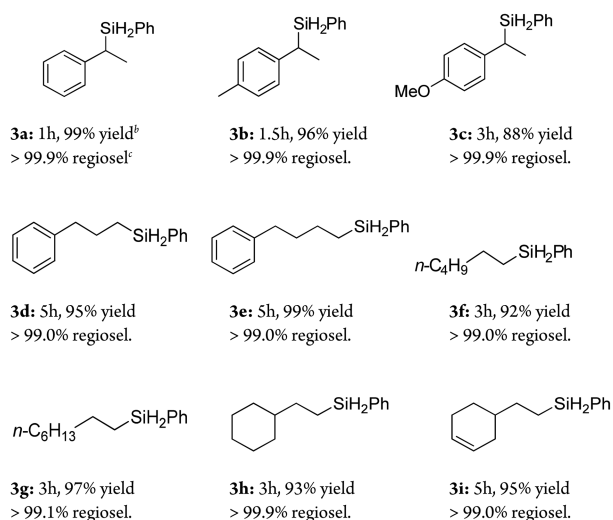
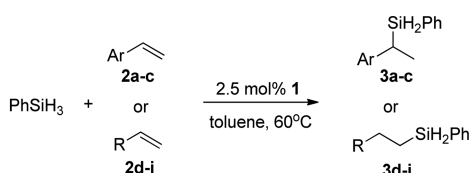
The isolation of **1** prompted us to investigate its potential for catalytic hydrosilylation reaction. Thus, the catalytic hydrosilylation of styrene with phenylsilane using complex **1** as catalyst has been examined. The results are summarized in Table 1. The reactions in THF at room temperature with 2.5 mol % loadings of **1** led to the formation of the hydrosilylation product with low conversions but the very good regioselectivity (>99.9%, entries 1). It can be seen in Table 1, the catalytic reaction in toluene is more efficient than those in donor solvents at room temperature (entries 1, 2 and 3) and the reaction at 60 °C resulted in a complete conversion in 1 h (entry 4). On the other hand, the reaction also proceeded with a good conversion (89%) under solvent-free conditions (entry 5). However, the decrease of the catalyst loading to 1.25 mol % led to a much low conversion (entry 6). Overall, the catalytic hydrosilylation of styrene using **1** in toluene at 60 °C is highly regioselective and efficient.

Encouraged by the initial results, various alkenes have been tested. It can be seen from Table 2 that **1** exhibited high

**Table 1. Optimization of the Hydrosilylation of Styrene with PhSiH<sub>3</sub> Catalyzed by 1<sup>a</sup>**

| entry          | solvent | T (°C) | convn (%) <sup>b</sup> | regioselectivity (%) <sup>c</sup> |
|----------------|---------|--------|------------------------|-----------------------------------|
| 1              | THF     | 23     | 31                     | >99.9                             |
| 2              | DME     | 23     | 12                     | >99.9                             |
| 3              | toluene | 23     | 43                     | >99.9                             |
| 4              | toluene | 60     | 100                    | >99.9                             |
| 5              | neat    | 60     | 89                     | >99.9                             |
| 6 <sup>d</sup> | toluene | 60     | 46                     | >99.9                             |

<sup>a</sup>Reactions were carried out on a scale of 1 mmol of phenylsilane and 1 mmol of styrene, in the presence of 2.5 mol % catalyst, in 1 mL of solvent for 1 h. <sup>b</sup>Conversion was estimated based on integration of the <sup>1</sup>H NMR spectrum. <sup>c</sup>The regioselectivity was analyzed by GC–MS of the crude reaction mixture. <sup>d</sup>In the presence of 1.25 mol % 1.

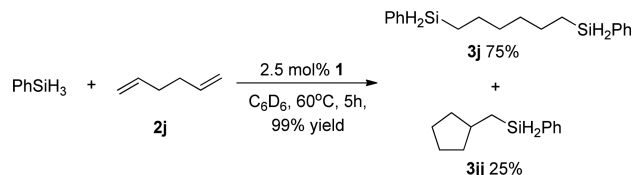
**Table 2. Results for the Hydrosilylation of Styrene Derivatives and Nonactivated Terminal Alkenes<sup>a</sup>**

<sup>a</sup>Reactions were carried out at 60 °C on a scale of 1 mmol of phenylsilane and 1 mmol of the appropriate alkene, in the presence of 2.5 mol % 1, in 1 mL of toluene. <sup>b</sup>Isolated yield. <sup>c</sup>The regioselectivity was analyzed by GC–MS of the crude reaction mixture.

regioselectivity (>99%) for both styrene derivatives and nonactivated terminal alkenes. The styrene derivatives 2a–2c were exclusively converted to the corresponding Markovnikov products 3a–3c in 88–99% yield, whereas nonactivated alkenes 2d–2i yielded anti-Markovnikov products 3d–3i in 92–99% yield. Both the <sup>1</sup>H NMR and gas chromatography–mass spectrometry (GC–MS) spectra of the crude products (see the Supporting Information, SI) indicated high regioselectivity. Hydrosilylation of nonconjugated diene 2i led to chemoselective silylation of the terminal C=C double bond, while the internal C=C bond remained intact with the formation of anti-Markovnikov product 3i in 95% yield. To the best of our knowledge, complex 1 is the most regioselective (>99.0%) rare-

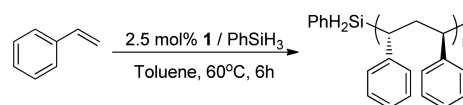
earth catalyst for both styrenes and nonactivated terminal alkenes reported so far.

It has been reported that hydrosilylation of 1,5-hexadiene (Scheme 2) catalyzed by rare-earth complexes may yield several

**Scheme 2. Hydrosilylation of Dienes with PhSiH<sub>3</sub> Catalyzed by 1**

products depending on the hydride or silyl intermediates.<sup>4b</sup> Hydrosilylation of 2j in C<sub>6</sub>D<sub>6</sub> catalyzed by 1 was monitored in an NMR tube. The reaction exclusively yielded 1,6-bis(phenylsilyl)hexane (3j) and (phenylsilylmethyl)cyclopentane (3jj; see the SI). The cyclization product 3jj has been proposed to be formed by the intramolecular alkene coordination–insertion into the Ln–C bond via a rare-earth hydride intermediate.<sup>4e,5a,d</sup> However, the product (3-methylcyclopentyl)phenylsilane, which was proposed to be formed via a rare-earth silyl intermediate, was not observed, indicating that the hydrosilylation reaction is likely to proceed via a rare-earth hydride intermediate.

To provide further evidence for the possible hydride intermediate, the polymerization of alkenes with 1 activated by PhSiH<sub>3</sub> was investigated. The polymerization of styrene cannot occur in the absence of PhSiH<sub>3</sub>. However, the addition of a small amount of PhSiH<sub>3</sub> to the precursor 1 led to the exclusive formation of polystyrene. 1 exhibited moderate activity at 60 °C with the formation of highly syndiotactic (>99%) silyl-capped polystyrene with moderate molecular weights (*M<sub>n</sub>* = 5100) and narrow molecular weight distribution (PDI = 1.33) under optimized conditions (Scheme 3). The

**Scheme 3. Synthesis of Highly Syndiotactic Silyl-Capped Polystyrene**

polymer has been characterized by <sup>1</sup>H, <sup>13</sup>C, and <sup>29</sup>Si NMR, gel permeation chromatography (GPC), and IR spectroscopy (see the SI). Syndiospecific polymerization of styrene has been realized with the single-component metallocene allyl catalysts (Flu-CMe<sub>2</sub>-Cp)Ln(C<sub>3</sub>H<sub>5</sub>)(THF) (Flu = fluorenyl; Cp = cyclopentadienyl; Ln = Y, La, Nd, and Sm) by Carpentier et al.<sup>20</sup> The half-sandwich cationic rare-earth alkyl complexes have also been reported by the Hou and Chen groups to be highly syndiospecific for styrene polymerization.<sup>21</sup> A number of rare-earth complexes have been reported to give syndio-rich polystyrenes.<sup>22</sup> However, no rare-earth alkoxides have been reported to be active precursors for polymerization of alkenes upon activation with hydrosilane.

In the <sup>1</sup>H NMR spectrum of the polymer, the characteristic PhSiH<sub>2</sub> resonance at 4.11 ppm indicated that the polymer was capped with a PhSiH<sub>2</sub> group. The intensity ratio of SiH<sub>2</sub>/CH<sub>3</sub> is 2:3, indicating the existence of only one silyl end group in the polymer chain. The resonance at –21.8 ppm and a strong

absorption at  $2130\text{ cm}^{-1}$  in the  $^{29}\text{Si}$  NMR and IR spectra, respectively, strongly support the silyl-capped polymers.<sup>23</sup> These spectroscopic features are consistent with those for the silyl-capped polystyrenes generated with a cationic Ziegler–Natta catalyst reported by Koo and Marks.<sup>24</sup> The syndiotacticity of the polymers was determined by the characteristic resonances in the  $^1\text{H}$  and  $^{13}\text{C}$  NMR spectra.<sup>20,21,25</sup> In the  $^{13}\text{C}$  NMR spectrum, the phenyl C-1 showed only four signals assigned to one major *rrrrrr* (at  $145.35\text{ ppm}$ ) and three minor *rrmrrr*, *rmrrrr*, and *mrmmrr* heptads (see the SI). The relative intensities of these signals are consistent with first-order Markovian (Bernoullian) statistics of a chain-end stereocontrol mechanism, giving a probability of *racemic* linkage between styrene units  $P_r$  of 0.89.<sup>26</sup> The  $M_n$  value determined by  $^1\text{H}$  NMR, based on the relative intensity of the resonances, is close to that determined by GPC standards ( $M_{n,\text{GPC}} = 5100$  and  $M_{n,\text{NMR}} = 4800$ ). To the best of our knowledge, this is the first example of a silyl-capped syndiotactic oligostyrene prepared directly by a polymerization process.

Temperatures have significant effects on the polymerization activity. At low temperatures, only a trace or a small amount of polymers was obtained (entries 1 and 2 in Table 3). High

**Table 3. Catalytic Styrene Polymerization by **1** in the Presence of  $\text{PhSiH}_3$ <sup>a</sup>**

| entry | $T$ (°C) | time (h) | solvent | $\text{PhSiH}_3$ (mmol) | yield (%) | $M_n$ <sup>b</sup> | PDI <sup>b</sup> |
|-------|----------|----------|---------|-------------------------|-----------|--------------------|------------------|
| 1     | 20       | 6        | toluene | 0.5                     | trace     |                    |                  |
| 2     | 40       | 6        | toluene | 0.5                     | 5         | 5000               | 2.00             |
| 3     | 60       | 6        | toluene | 0.5                     | 71        | 5100               | 1.33             |
| 4     | 60       | 2        | toluene | 0.5                     | 38        | 4800               | 1.16             |
| 5     | 60       | 4        | toluene | 0.5                     | 55        | 5200               | 1.26             |
| 6     | 60       | 6        | THF     | 0.5                     | trace     |                    |                  |
| 7     | 60       | 6        | bulk    | 0.5                     | 61        | 4900               | 1.22             |
| 8     | 60       | 6        | toluene | 0.1                     | 53        | 11200              | 1.84             |
| 9     | 60       | 6        | toluene | 0.2                     | 60        | 7800               | 1.61             |
| 10    | 60       | 6        | toluene | 0.8                     | 42        | 4200               | 1.07             |
| 11    | 60       | 6        | toluene | 1.0                     | 35        | 3800               | 1.01             |

<sup>a</sup>Polymerization conditions: **1** (0.0125 mmol), styrene (5 mmol, 0.58 mL),  $\text{PhSiH}_3$  (0.5 mmol), toluene (0.5 mL). <sup>b</sup>Determined by GPC in THF at  $25\text{ }^\circ\text{C}$  against a polystyrene standard,  $\text{PDI} = M_w/M_n$ .

activity was achieved at  $60\text{ }^\circ\text{C}$  (entry 3). The prolonged polymerization time resulted in an increase of the yields, but the molecular weights remained in the range of 4800–5200 (entries 3–5). In addition, donor solvents such as THF significantly suppressed the reaction (entry 6) probably because of the competition of the coordination of the solvent with that of styrene. Bulk polymerization of styrene also proceeded with a good yield (entry 7). The effects of the amount of  $\text{PhSiH}_3$  on the catalytic performances have also been studied. With an increase of  $[\text{PhSiH}_3]$ , the molecular weights decreased (entries 3 and 8–11), suggesting that the polymer chain is likely to be terminated by  $\text{PhSiH}_3$ . This result is consistent with the proposed samarium hydride intermediate.

The mechanisms for hydrosilylation and stereospecific polymerization have been investigated experimentally and theoretically. The addition of **1** to a 15-fold molar excess of  $\text{PhSiH}_3$  in  $\text{C}_6\text{D}_6$  led to the formation of a small amount (ca. 3% conversion based on  $\text{PhSiH}_3$ ) of  $\text{Ph}_2\text{SiH}_2$  and  $\text{SiH}_4$ , indicating that  $\sigma$ -bond metathesis with the silane occurred to some extent.<sup>7b</sup> It is likely that complex **1** reacted with  $\text{PhSiH}_3$  to form

active samarium species by  $\sigma$ -bond metathesis of the  $\text{Sm}-\text{O}$  bond.  $\sigma$ -bond metathesis of some transition-metal alkoxides with hydrosilanes to yield the metal hydride is known.<sup>9</sup> However, these types of reactions have not been reported for rare-earth alkoxides.

Kinetic studies on the hydrosilylation of 1-hexene were operated in  $\text{C}_6\text{D}_6$  and recorded by  $^1\text{H}$  NMR spectroscopy. They indicated that the rate law of hydrosilylation was of first-order dependence on **1** and 1-hexene but of zero-order on  $\text{PhSiH}_3$  (Figures 2 and 3 and Tables S1 and S2 in the SI). The

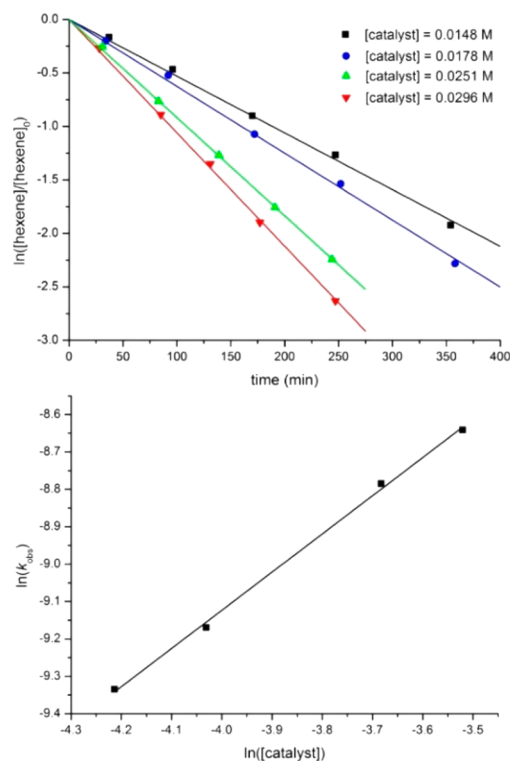


**Figure 2.** (above) Kinetic plots for the catalytic  $\text{PhSiH}_3$  hydrosilylation of 1-hexene as a function of the indicated catalyst concentrations. Initial  $[\text{hexene}] = 0.5\text{ M}$  and  $[\text{PhSiH}_3] = 5\text{ M}$ . (below) Dependence of the observed rate constants for the hydrosilylation process in the kinetic plots (above) on the catalyst concentration. The linear relationship has a slope of 1.02093.

results suggested that the active catalytic species is a mononuclear intermediate in the catalytic cycle, and 1-hexene might be involved in the rate-determining step.

Taking the preliminary mechanistic studies into account, we propose an insertion/metathesis mechanism involving active samarium hydride species (Figure 4). Complex **1** may dissociate in solution and underwent  $\sigma$ -bond metathesis of **1** with  $\text{PhSiH}_3$  to yield samarium hydride. The subsequent coordination–insertion of an alkene led to the  $\text{Sm}-\text{C}$  intermediate, which reacted with  $\text{PhSiH}_3$  to give the product and regenerate the samarium hydride intermediate.<sup>4–6</sup> The continuous insertion of styrene into the  $\text{Sm}-\text{C}$  bond resulted in chain growth to form polymers, which was terminated by  $\sigma$ -bond metathesis with  $\text{PhSiH}_3$  to yield the silyl-capped polystyrenes and samarium hydride intermediate.<sup>27</sup>

To gain further support for the proposed mechanism, DFT calculations were performed on the model reaction of the hydrosilylation of propene with  $\text{PhSiH}_3$  (Figure S4,b). In the initial catalyst activation stage, a samarium hydride intermedi-

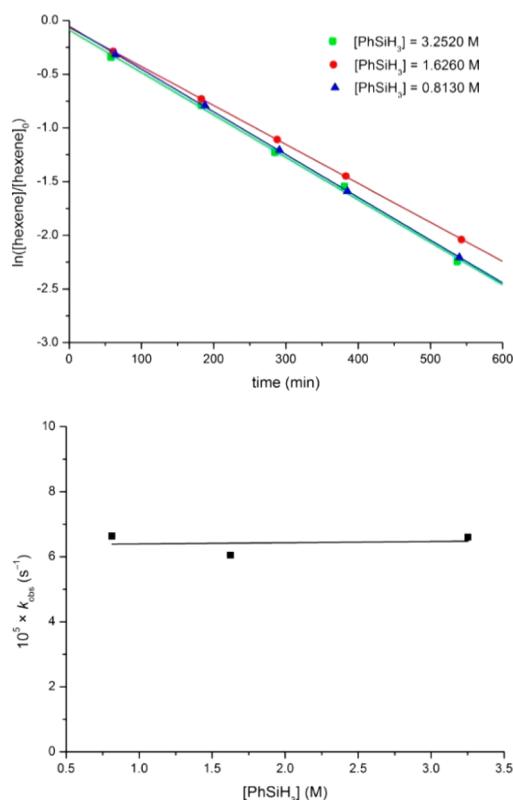


**Figure 3.** (above) Kinetic plots for the catalytic  $\text{PhSiH}_3$  hydrosilylation of 1-hexene over the indicated range of  $\text{PhSiH}_3$  concentrations. Initial  $[\text{hexene}] = 0.5 \text{ M}$  and  $[\text{catalyst}] = 0.012 \text{ M}$ . (below) Dependence of the observed rate constants for the hydrosilylation process in the kinetic plots (above) on the  $\text{PhSiH}_3$  concentration. The linear relationship has a slope of 0.03672.

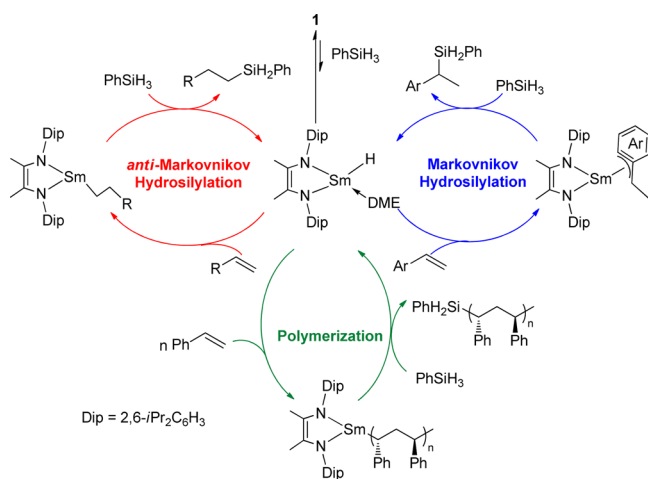


**Figure 4.** Proposed mechanism of hydrosilylation and polymerization.

ate,  $\text{LSmH}(\text{DME})$  (**A**), is formed by  $\sigma$ -bond metathesis of **4** with  $\text{PhSiH}_3$  via the transition state **TS**, requiring an activation free energy of 29.4 kcal/mol. The subsequent primary coordination of propene to the samarium atom led to the intermediate **A'**, which underwent 1,2-insertion via the 4-centered transition state **R-TS1-L** with an energy barrier of 25.8 kcal/mol to give the alkyl intermediate **B**. Subsequently, the intermediate **B** underwent  $\sigma$ -bond metathesis with  $\text{PhSiH}_3$  via the 4-centered transition state **R-TS2-L** with an energy barrier of 19.5 kcal/mol to produce the silane  $\sigma$  intermediate **B'**.

Finally, the release of the hydrosilylation product from **B'** by exchange with DME regenerated the hydride **A**. The insertion step has the highest energy barrier and thus is the rate-determining step, consistent with the kinetic studies.<sup>4e</sup>

The regioselectivity of hydrosilylation depends on the coordination–insertion modes. The calculated results are shown in Figure 5c. The primary 1,2-coordination–insertion of a propene molecule is favored over the secondary 2,1-coordination–insertion by 2.6 kcal/mol because of the stronger steric repulsion between the terminal alkene substituent and the bulky ene-diamido ligand in **R-TS1-B** than in **R-TS1-L**. This is consistent with the observed regioselectivity for nonactivated alkenes. With regard to the hydrosilylation of styrene, the 2,1-coordination–insertion is much favored by 7.8 kcal/mol over the 1,2 mode because of the stabilizing  $\eta^3$  binding of styrene to the samarium atom in **Ph-TS1-B** (Figure 5d), leading to the Markovnikov products exclusively. Maron and co-workers have analyzed the energy profiles for the  $\text{Cp}_2\text{SmH}$ -catalyzed ( $\text{Cp} = \text{C}_5\text{H}_5$ ) hydrosilylation of propene with  $\text{SiH}_4$ , and their calculations support the  $\text{Cp}_2\text{SmSiH}_3$  mechanism.<sup>28</sup> It can be concluded that both the bulky ene-diamido ligand and the  $\text{Sm-O}$  bond play important roles for the hydride intermediate and observed selectivity.

In the chain growth of polymerization, the insertion of styrene into the  $\text{LSmCH}(\text{Me})\text{Ph}$  intermediate requires an activation free energy of 23.8 kcal/mol based on calculations (see Figure S1 in the SI), which suggests that polymerization of styrene is feasible in the experimental conditions. The solvent effects observed in the catalytic system are in accordance with the coordination–insertion mechanism.

We also considered the possible reaction mechanism involved in the samarium silyl intermediate (see pathway II in Figure S2 in the SI). In pathway II, the silyl complex (**C**) generated by the reaction of  $\text{PhSiH}_3$  with **4** requires a total free energy of 49.0 kcal/mol. Therefore, this mechanism could be ruled out because of the very high energy barrier.

## CONCLUSION

In summary, we have disclosed the first ene-diamido rare-earth alkoxide complex that is capable of catalyzing both the regioselective (>99%) hydrosilylation of terminal alkenes and the syndiospecific polymerization of styrene with the selective and clean formation of valuable secondary silanes in high yields and novel silyl-capped syndiotactic oligostyrenes. The molecular weights of the polymers can be adjusted by variation of the amount of phenylsilane. It has been observed that hydrosilylation and polymerization with other silanes such as  $n\text{-BuSiH}_3$ ,  $\text{Ph}_2\text{SiH}_2$ , and  $\text{Ph}_3\text{SiH}$  did not occur under our catalytic conditions. DFT calculations strongly support the formation of a samarium hydride intermediate via  $\sigma$ -bond metathesis of the  $\text{Sm-O}$  bond in **1** with  $\text{PhSiH}_3$ . The high regioselectivity observed for the hydrosilylation reaction is due to the unique steric and electronic factors of the ene-diamido ligand and the formation of the hydride intermediate. The formation of the hydride intermediate was also supported by the hydrosilylation of 1,5-hexadiene and the formation of silyl-capped polystyrene. The results demonstrated that more stable rare-earth alkoxides could be used for hydrosilylation and styrene polymerization reactions. The development of highly active rare-earth alkoxide precatalysts for the hydroelementation of unsaturated species are currently underway in our laboratory.

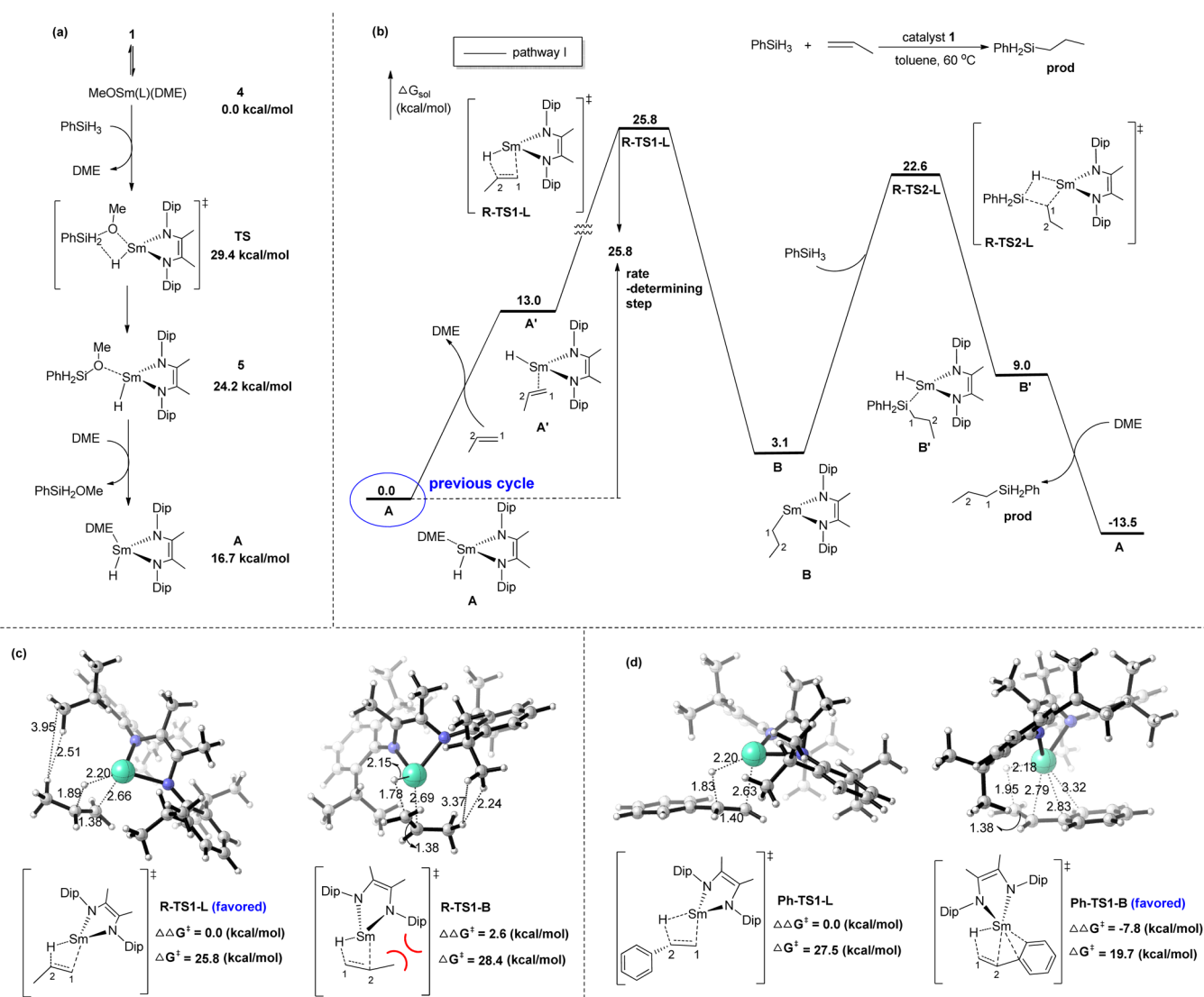


**Figure 5.** (a) Mechanism for the formation of the active catalyst A. (b) Gibbs free-energy profile of the 1-catalyzed hydrosilylation of propene. Energies are calculated using the M06/ECP51MWB-6-311+G(d,p)/SMD(toluene)//B3LYP/ECP51MWB-6-31G(d) method. (c) TS structures and relative free energies for the regioselectivity-determining insertion of propene. (d) TS structures and relative free energies for the regioselectivity-determining insertion of styrene.

## ASSOCIATED CONTENT

### Supporting Information

The Supporting Information is available free of charge on the ACS Publications website at DOI: 10.1021/acs.inorgchem.6b01670.

Experimental, crystallographic, and computational details (PDF)

Crystallographic data for 1 in CIF format (CIF)

## AUTHOR INFORMATION

### Corresponding Authors

\*E-mail: xxfang@nankai.edu.cn.

\*E-mail: cmcui@nankai.edu.cn.

### Notes

The authors declare no competing financial interest.

## ACKNOWLEDGMENTS

We are grateful to the National Natural Science Foundation of China and 973 program (Grants 2012CB821600, 21390401,

21421001), Natural Science Foundation of Tianjin (Grant 16JCQNJC05800), and MOE Innovation Teams (IRT-13R30 and IRT13022) of China for financial support.

## REFERENCES

- (1) Edlmann, F. T. In *Comprehensive Organometallic Chemistry III*; Crabtree, R. H., Mingos, D. M. P., Eds.; Elsevier: Oxford, U.K., 2007; Vol. 4.
- (2) (a) Molander, G. A.; Romero, J. A. C. *Chem. Rev.* **2002**, *102*, 2161–2186. (b) Marciniak, B.; Maciejewski, H.; Pietraszuk, C.; Pawluć, P. In *Hydrosilylation: a Comprehensive Review on Recent Advances*; Marciniak, B., Eds.; Springer: Berlin, Germany, 2009.
- (3) (a) Nishiura, M.; Guo, F.; Hou, Z. *Acc. Chem. Res.* **2015**, *48*, 2209–2220. (b) Gromada, J.; Carpentier, J.-F.; Mortreux, A. *Coord. Chem. Rev.* **2004**, *248*, 397–410. (c) Takeuchi, D. *Dalton Trans.* **2010**, 39, 311–328.
- (4) Rare-earth alkyl complexes: (a) Sakakura, T.; Lautenschläger, H.-J.; Tanaka, M. *J. Chem. Soc., Chem. Commun.* **1991**, 40–41. (b) Fu, P.-F.; Brard, L.; Li, Y.; Marks, T. J. *J. Am. Chem. Soc.* **1995**, *117*, 7157–7168. (c) Molander, G. A.; Retsch, W. H. *J. Am. Chem. Soc.* **1997**, *119*, 8817–8825. (d) Gountchev, T. I.; Tilley, T. D. *Organometallics* **1999**,

- 18, 5661–5667. (e) Konkol, M.; Kondracka, M.; Voth, P.; Spaniol, T. P.; Okuda, J. *Organometallics* **2008**, *27*, 3774–3784. (f) Trambitas, A. G.; Panda, T. K.; Jenter, J.; Roesky, P. W.; Daniliuc, C.; Hrib, C. G.; Jones, P. G.; Tamm, M. *Inorg. Chem.* **2010**, *49*, 2435–2446. (g) Molander, G. A.; Julius, M. *J. Org. Chem.* **1992**, *57*, 6347–6351. (h) Molander, G. A.; Dowdy, E. D.; Noll, B. C. *Organometallics* **1998**, *17*, 3754–3758. (i) Molander, G. A.; Corrette, C. P. *Organometallics* **1998**, *17*, 5504–5512. (j) Molander, G. A.; Knight, E. E. *J. Org. Chem.* **1998**, *63*, 7009–7012. (k) Robert, D.; Trifonov, A. A.; Voth, P.; Okuda, J. *J. Organomet. Chem.* **2006**, *691*, 4393–4399. (l) Fu, P.-F. *J. Mol. Catal. A: Chem.* **2006**, *243*, 253–257. (m) Elvidge, B. R.; Arndt, S.; Spaniol, T. P.; Okuda, J. *Dalton Trans.* **2006**, 890–901. (n) Abinet, E.; Spaniol, T. P.; Okuda, J. *Chem. - Asian J.* **2011**, *6*, 389–391.
- (5) Rare-earth hydride complexes: (a) Ohashi, M.; Konkol, M.; Del Rosal, I.; Poteau, R.; Maron, L.; Okuda, J. *J. Am. Chem. Soc.* **2008**, *130*, 6920–6921. (b) Ruspica, C.; Spielmann, J.; Harder, S. *Inorg. Chem.* **2007**, *46*, 5320–5326. (c) Muci, A. R.; Bercaw, J. E. *Tetrahedron Lett.* **2000**, *41*, 7609–7612. (d) Trifonov, A. A.; Spaniol, T. P.; Okuda, J. *Dalton Trans.* **2004**, 2245–2250.
- (6) Rare-earth amide complexes: (a) Takaki, K.; Sonoda, K.; Kousaka, T.; Koshiji, G.; Shishido, T.; Takehira, K. *Tetrahedron Lett.* **2001**, *42*, 9211–9214. (b) Takaki, K.; Komeyama, K.; Takehira, K. *Tetrahedron* **2003**, *59*, 10381–10395. (c) Rastätter, M.; Zulus, A.; Roesky, P. W. *Chem. Commun.* **2006**, 874–876. (d) Ruspica, C.; Spielmann, J.; Harder, S. *Inorg. Chem.* **2007**, *46*, 5320–5326. (e) Horino, Y.; Livinghouse, T. *Organometallics* **2004**, *23*, 12–14. (f) Rastätter, M.; Zulus, A.; Roesky, P. W. *Chem. - Eur. J.* **2007**, *13*, 3606–3616.
- (7) (a) Malanga, M. *Adv. Mater.* **2000**, *12*, 1869–1872. (b) Castillo, I.; Tilley, T. D. *J. Am. Chem. Soc.* **2001**, *123*, 10526–10534. (c) Sadow, A. D.; Tilley, T. D. *Angew. Chem., Int. Ed.* **2003**, *42*, 803–805. (d) Radu, N. S.; Tilley, T. D.; Rheingold, A. L. *J. Am. Chem. Soc.* **1992**, *114*, 8293–8295.
- (8) Nolan, S. P.; Stern, D.; Marks, T. J. *J. Am. Chem. Soc.* **1989**, *111*, 7844–7853.
- (9) For example, see: (a) Mimoun, H.; de Saint Laumer, J. Y.; Giannini, L.; Scopelliti, R.; Floriani, C. *J. Am. Chem. Soc.* **1999**, *121*, 6158–6166. (b) Sattler, W.; Parkin, G. *J. Am. Chem. Soc.* **2012**, *134*, 17462–17465. (c) Kahnes, M.; Görls, H.; Gonzalez, L.; Westerhausen, M. *Organometallics* **2010**, *29*, 3098–3108. (d) Chu, W.-Y.; Zhou, X.; Rauchfuss, T. B. *Organometallics* **2015**, *34*, 1619–1626. (e) Bleith, T.; Gade, L. H. *J. Am. Chem. Soc.* **2016**, *138*, 4972–4983. (f) Mukherjee, D.; Thompson, R. R.; Ellern, A.; Sadow, A. D. *ACS Catal.* **2011**, *1*, 698–702. (g) Tran, B. L.; Pink, M.; Mindiola, D. J. *Organometallics* **2009**, *28*, 2234–2243. (h) Chakraborty, S.; Krause, J. A.; Guan, H. *Organometallics* **2009**, *28*, 582–586. (i) Pirnot, M. T.; Wang, Y.-M.; Buchwald, S. L. *Angew. Chem., Int. Ed.* **2016**, *55*, 48–57.
- (10) Lohr, T. L.; Li, Z.; Marks, T. J. *Acc. Chem. Res.* **2016**, *49*, 824–834.
- (11) Cui, D.; Nishiura, M.; Tardif, O.; Hou, Z. *Organometallics* **2008**, *27*, 2428–2435.
- (12) (a) Trifonov, A. A.; Fedorova, E. A.; Fukin, G. K.; Druzhkov, N. O.; Bochkarev, M. N. *Angew. Chem., Int. Ed.* **2004**, *43*, 5045–5048. (b) Vasudevan, K.; Cowley, A. H. *Chem. Commun.* **2007**, 3464–3466. (c) Panda, T. K.; Kaneko, H.; Pal, K.; Tsurugi, H.; Mashima, K. *Organometallics* **2010**, *29*, 2610–2615. (d) Shestakov, B. G.; Mahrova, T. V.; Larionova, J.; Long, J.; Cherkasov, A. V.; Fukin, G. K.; Lyssenko, K. A.; Scherer, W.; Hauf, C.; Magdesieva, T. V.; Levitskiy, O. A.; Trifonov, A. A. *Organometallics* **2015**, *34*, 1177–1185.
- (13) Mahrova, T. V.; Fukin, G. K.; Cherkasov, A. V.; Trifonov, A. A.; Ajellal, N.; Carpentier, J.-F. *Inorg. Chem.* **2009**, *48*, 4258–4266.
- (14) Kaneko, H.; Nagae, H.; Tsurugi, H.; Mashima, K. *J. Am. Chem. Soc.* **2011**, *133*, 19626–19629.
- (15) Kissel, A. A.; Mahrova, T. V.; Lyubov, D. M.; Cherkasov, A. V.; Fukin, G. K.; Trifonov, A. A.; Del Rosal, I.; Maron, L. *Dalton Trans.* **2015**, *44*, 12137–12148.
- (16) Li, J.; Huang, H.; Wang, F.; Cui, C. *Organometallics* **2015**, *34*, 683–685.
- (17) Gans-Eichler, T.; Gudat, D.; Nättinen, K.; Nieger, M. *Chem. - Eur. J.* **2006**, *12*, 1162–1173.
- (18) (a) Evans, W. J.; Ulibarri, T. A.; Ziller, J. W. *Organometallics* **1991**, *10*, 134–142. (b) Deelman, B.-J.; Booij, M.; Meetsma, A.; Teuben, J. H.; Kooijman, H.; Spek, A. L. *Organometallics* **1995**, *14*, 2306–2317. (c) Marchetti, F.; Pampaloni, G.; Zacchini, S. *Chem. Commun.* **2008**, 3651–3653. (d) Liu, B.; Liu, X.; Cui, D.; Liu, L. *Organometallics* **2009**, *28*, 1453–1460. (e) Tolpygin, A. O.; Shavyrin, A. S.; Cherkasov, A. V.; Fukin, G. K.; Trifonov, A. A. *Organometallics* **2012**, *31*, 5405–5413. (f) Kissel, A. A.; Lyubov, D. M.; Mahrova, T. V.; Fukin, G. K.; Cherkasov, A. V.; Glukhova, T. A.; Cui, D.; Trifonov, A. A. *Dalton Trans.* **2013**, *42*, 9211–9225.
- (19) (a) Duncalf, D. J.; Hitchcock, P. B.; Lawless, G. A. *Chem. Commun.* **1996**, 269–271. (b) Gun'ko, Y. K.; Hitchcock, P. B.; Lappert, M. F. *J. Organomet. Chem.* **1995**, *499*, 213–219. (c) Cristina Cassani, M.; Lappert, M. F.; Laschi, F. *Chem. Commun.* **1997**, 1563–1564. (d) Deacon, G. B.; Junk, P. C.; Moxey, G. J. *Z. Anorg. Allg. Chem.* **2008**, *634*, 2789–2792. (e) Liddle, S. T.; Arnold, P. L. *Dalton Trans.* **2007**, 3305–3313. (f) Arnold, P. L.; Liddle, S. T. *Organometallics* **2006**, *25*, 1485–1491.
- (20) (a) Kirillov, E.; Lehmann, C. W.; Razavi, A.; Carpentier, J.-F. *J. Am. Chem. Soc.* **2004**, *126*, 12240–12241. (b) Rodrigues, A.-S.; Kirillov, E.; Lehmann, C. W.; Roisnel, T.; Vuillemin, B.; Razavi, A.; Carpentier, J.-F. *Chem. - Eur. J.* **2007**, *13*, 5548–5565.
- (21) (a) Luo, Y.; Baldamus, J.; Hou, Z. *J. Am. Chem. Soc.* **2004**, *126*, 13910–13911. (b) Nishiura, M.; Mashiko, T.; Hou, Z. *Chem. Commun.* **2008**, 2019–2021. (c) Jaroschik, F.; Shima, T.; Li, X.; Mori, K.; Ricard, L.; Le Goff, X.-F.; Nief, F.; Hou, Z. *Organometallics* **2007**, *26*, 5654–5660. (d) Xu, X.; Chen, Y.; Sun, J. *Chem. - Eur. J.* **2009**, *15*, 846–850.
- (22) (a) Rodrigues, A.-S.; Kirillov, E.; Carpentier, J.-F. *Coord. Chem. Rev.* **2008**, *252*, 2115–2136. (b) Schellenberg, J. *Prog. Polym. Sci.* **2009**, *34*, 688–718.
- (23) (a) Pawlenko, S. *Organosilicon Chemistry*; Walter de Gruyter: New York, 1986. (b) Crompton, J. R. In *The Chemistry of Organic Silicon Compounds*; Patai, S., Rappoport, Z., Eds.; John Wiley: Chichester, U.K., 1984.
- (24) Koo, K.; Marks, T. J. *J. Am. Chem. Soc.* **1999**, *121*, 8791–8802.
- (25) (a) Rodrigues, A.-S.; Kirillov, E.; Vuillemin, B.; Razavi, A.; Carpentier, J.-F. *J. Mol. Catal. A: Chem.* **2007**, *273*, 87–91. (b) Sarazin, Y.; de Frémont, P.; Annunziata, L.; Duc, M.; Carpentier, J.-F. *Adv. Synth. Catal.* **2011**, *353*, 1367–1374.
- (26) (a) Feil, F.; Harder, S. *Macromolecules* **2003**, *36*, 3446–3448. (b) Busico, V.; Cipullo, R. *Prog. Polym. Sci.* **2001**, *26*, 443–533.
- (27) Fu, P.-F.; Marks, T. J. *J. Am. Chem. Soc.* **1995**, *117*, 10747–10748.
- (28) (a) Barros, N.; Eisenstein, O.; Maron, L. *Dalton Trans.* **2010**, *39*, 10749–10756. (b) Barros, N.; Eisenstein, O.; Maron, L. *Dalton Trans.* **2010**, *39*, 10757–10767.